Inorganic Chemistry
Article

Inorg. Chem. **2010**, *49*, 3019–3024 **3019**
DOI: 10.1021/ic9025552

Synthesis, Magnetic Structure, and Properties of a Layered Cobalt−Hydroxide Ferromagnet, $Co_5(OH)_6(SeO_4)_2(H_2O)_4$

Wassim Maalej,[†] Serge Vilminot,*[,†] Gilles André,[‡] and Mohamedally Kurmoo*[,§]

[†]*Département Chimie des Matériaux Inorganiques, IPCMS, UMR 7504 (CNRS-UDS), 23 rue du Loess, BP 43, 67034 Strasbourg Cedex 2, France,* [‡]*Laboratoire Léon Brillouin, CEA-CNRS, CEA Saclay, 91191 Gif sur Yvette Cedex, France, and* [§]*Laboratoire de Chimie de Coordination Organique, CNRS-UMR 7140, Université de Strasbourg, Institut Le Bel, 4 rue Blaise Pascal, 67000 Strasbourg Cedex 01, France*

Received December 22, 2009

The synthesis and nuclear and magnetic structures from the powder diffraction of $Co^{II}_5(OH)_6(SeO_4)_2(H_2O)_4$ and its deuterated analogues as well as their infrared spectral, thermal, and magnetic properties are reported. The nuclear structure consists of brucite-like cobalt hydroxide layers connected by ...$OSeO_3$−$Co(H_2O)_4$−O_3SeO... bridges. The two independent cobalt atoms within the layer are arranged in chains along the *b* axis creating an anisotropy within each layer. The interlayer distance (10.718 Å) is the only parameter to increase compared to the sulfate analogue (10.273 Å). The infrared spectra and thermal properties are similar to those reported for the sulfate analogue. Due to the ferromagnetic exchange between the nearest-neighbor cobalt atoms within the layer, satisfying the Good-enough−Kanamori rule, and the weak interlayer exchange, an overall ferromagnet is obtained. The ferromagnetic order at 9 K was confirmed by the ac susceptibilities, the saturation magnetization, and most importantly the enhancement of some Bragg diffraction peaks below the Curie temperature. The moments of all the cobalt atoms were found to be aligned along the *b* axis with a moment of 3.25(8) μ_B each giving the best fit. The increase in layer distance and the electron density by replacing sulfur by selenium lowers the Curie temperature.

Introduction

Ferromagnetism is a rarely observed phenomenon as it requires all the moments on every site to be parallel, thus requiring the very rare occurrence of no overlapping between magnetic orbitals of nearest neighbor moment carriers.[1] This is possible only if the magnetic orbitals are orthogonal to each other. In contrast, antiferromagnetism is most favorable, as there is enough overlap between orbitals from nearest neighbors in most cases that pairing of the electrons takes place.[2] One way around this problem for making magnets is to use different moment carriers in ordered magnetic sublattices giving rise to ferrimagnetism.[3] Nature seems to have realized this first by the natural formation of loadstone, ferrite Fe_3O_4, which contains three magnetic sublattices with a resultant uncompensated moment.[1,4] However, there are very few cases where ferromagnetic alignment is favored. One of them is when two cobalt(II) atoms share an edge.[5] If this is extended in three dimensions, one expects all the moments to be parallel, thus generating a ferromagnet. This particular arrangement has not been realized yet. However, it is well-known for layers where edge-sharing can satisfy all the structural conditions, as in the layered hydroxide adopting the brucite, $Mg(OH)_2$, structure.[6] Therefore, $Co(OH)_2$ has been found to consist of ferromagnetic layers, but in this particular case, the interaction between layers is antiferromagnetic, which consequently resulted in a fully compensated antiferromagnet at T_N of 10 ± 1 K.[7] This particular layered structure is very rare and is known in only two other

*To whom correspondence should be addressed. Fax: 00 33 3 88 10 72 47 (S.V.); 00 33 3 68 85 13 25 (M.K.). E-mail: vilminot@ipcms.u-strasbg.fr (S.V.); kurmoo@chimie.u-strasbg.fr (M.K.).

(1) (a) Morrish, A. H. *The Physical Principles of Magnetism*; R. E. Krieger: Huntington, NY, 1980. (b) Chikazumi, S. *Physics of Ferromagnetism*; Clarendon Press: Oxford, U. K., 1997. (c) Herpin, A. *Théorie du Magnétisme*; Presse Universitaires de France: Paris, 1968. (d) Blundell, S. J. *Magnetism in Condensed Matter*; Oxford University Press: Oxford, U. K., 2001. (e) Carlin, R. L. *Magnetochemistry*; Springer: Berlin, 1986. (f) Day, P. *J. Chem. Soc., Dalton Trans.* **1997**, 701.

(2) Néel, L. *Ann. Phys.* **1948**, *1*, 137.

(3) (a) *Molecular Magnetism, New Magnetic Materials*; Itoh, K., Kinoshita, M., Ed.; Gordon Breach-Kodansha: Tokyo, 2000. (b) *Metal−Organic and Organic Molecular Magnets*; Day, P., Underhill, A. E., Eds.; Special Publication, Royal Society of Chemistry: Cambridge, UK, 2000; vol. *252*. (c) Blundell, S. J.; Pratt, F. L. *J. Phys.: Condens. Matter* **2004**, *16*, R771.

(4) *Magnetism Fundamentals* du Trémolet de Lacheisserie, É., Gignoux, D., Schelenker, M., Eds; Springer: New York, 2005; Chapter 1.

(5) Kurmoo, M. *Chem. Soc. Rev.* **2009**, *38*, 1353.

(6) (a) Zigan, F.; Rothbauer, R. *Neues Jahrb. Mineral Monatsh* **1967**, 137. (b) Parise, J. B.; Leinenweber, K.; Weidner, D. J.; Tan, K.; Von Dreele, R. B. *Am. Mineral.* **1994**, *79*, 193.

(7) (a) Takada, T.; Bando, Y.; Kiyama, M.; Myamoto, H.; Sato, T. *J. Phys. Soc. Jpn.* **1966**, *21*, 2726. (b) Sorai, M.; Kosaki, A.; Suga, H.; Seki, S. *J. Chem. Thermodyn.* **1969**, *1*, 119.

Published on Web 02/12/2010

compounds, $Co_2(OH)_3NO_3$ and $Co_5(OH)_6(SO_4)_2(H_2O)_4$.[8,9] The former contains similar CoO_2 layers, but one in four of the hydroxide oxygen atoms is replaced by one of the nitrates. Therefore, the interlayer distance is increased from 4.7 Å for $Co(OH)_2$ to 6.95 Å for $Co_2(OH)_3NO_3$. The interaction between layers is still antiferromagnetic, and the Néel temperature is 10 ± 1 K, which is not much perturbed by the increase in interlayer distance and the presence of NO_3 in the gallery.[8] Because the interlayer exchange is weak, a moderate magnetic field of less than 2 kOe is enough to easily reverse the moments in all the layers to be parallel. $Co_5(OH)_6(SO_4)_2(H_2O)_4$, on the other hand, consists of a bridge between the layers where the connector is $...OSO_3-Co(H_2O)_4-O_3SO...$ resulting in an interlayer spacing of 10.3 Å. Interestingly it is the first ferromagnet in the cobalt−hydroxide series. Extensive magnetic and neutron scattering measurements reveal that the moments within the layer are ordered first at 14 K, and thermodynamic measurements indicate that of the bridge becomes ordered at lower temperatures suggesting that this particular material behaves as a single-layer magnet within a limited range of temperatures.[9] The nuclear structure is the same at all temperatures between 1.6 and 300 K, and the magnetic structure has all the moments lying within the layer along the *b* axis. This characteristic may be associated with the very weak magnetic interaction between layers. These peculiar behaviors prompted us to study the selenate analogue, $Co_5(OH)_6(SeO_4)_2(H_2O)_4$, to understand the effect of introducing an electronically more dense element (selenium) in the place of the less dense one (sulfur) as well as modifying the interlayer distance. Here, we report the synthesis, its nuclear and magnetic structures, and its magnetic properties as part of our interest in the magnetic properties of synthetic minerals.[10−12] It is a ferromagnet with a slightly lower Curie temperature than the sulfate, and the neutron scattering reveals ordering of all the moments along the *b* axis.

Experimental Section

Synthesis. The starting material $CoSeO_4 \cdot 5H_2O$ was first prepared by the reaction of cobalt(II) carbonate hydrate (Aldrich, 45 wt % Co) and selenic acid H_2SeO_4 (Aldrich, 40 wt % water solution). The resulting red solution was evaporated yielding red crystals of $CoSeO_4 \cdot 5H_2O$ that were then ground to a pink powder before further use. $CoSeO_4 \cdot 5H_2O$ (1.2 g, 4.11 mmol) and NaOH (0.10 g, 2.5 mmol) were separately dissolved in 15 mL of deoxygenated boiling distilled water. The two solutions were mixed to give a blue suspension that was immediately poured in a Teflon-lined stainless steel bomb of 125 cm^3 capacity and heated at 150 °C for 48 h. After cooling, the pink microcrystals of $Co_5(OH)_6(SeO_4)_2(H_2O)_4$ (**1H**) having a platelet habit were decanted and washed with water, ethanol, and acetone before drying at 40 °C. For powder neutron diffraction, the deuterated compound **1D** was prepared using the same procedure as above but replacing H_2O by D_2O. Deuterium has a low incoherent neutron scattering factor compared to hydrogen and thus results in a reduction of the background.

Characterizations. Infrared spectra were recorded by transmission through KBr pellets containing 1% of the crystals using a Digilab Excalibur Series FTIR spectrometer. TG-DTA analyses were performed on a TGA92 Setaram apparatus under air at a heating rate of 5 °C/min in a platinum crucible. Powder X-ray diffraction patterns were recorded using a D8 Bruker diffractometer (Cu $K\alpha_1$, 1.5406 Å), equipped with a front monochromator. EDX analyses were performed using a Kevex unit of a Jeol 6700 F SEM apparatus. Magnetization measurements were performed in the temperature range 2−300 K and a field up to 50 kOe by means of a Quantum Design MPMS-XL SQUID magnetometer.

The neutron diffraction experiments were performed at the Laboratoire Léon Brillouin (CEA Saclay) using the multidetector (800 cells) G4.1 ($\lambda = 2.4226$ Å) diffractometer for the determination of the magnetic structure and the thermal evolution study of the low temperature patterns. Thirteen diffraction patterns were recorded in the 2θ range 2−82°, at different temperatures between 1.5 and 12 K. The powder sample was set in a cylindrical vanadium can and held in a liquid helium cryostat. Nuclear and magnetic structures were refined using the FULLPROF program.[13] The nuclear scattering lengths ($b_{Co} = 0.2490 \times 10^{-12}$ cm, $b_{Se} = 0.7970 \times 10^{-12}$ cm, $b_O = 0.5803 \times 10^{-12}$ cm, $b_D = 0.6671 \times 10^{-12}$ cm, $b_H = -0.3739 \times 10^{-12}$ cm) and cobalt(II) magnetic form factor were those included in this program.

Results and Discussion

Synthesis. Although it has been possible to make the desired compounds, **1H** and **1D**, it has been difficult to obtain them as pure phases. There is always the presence of a small quantity of the corresponding anhydrous compound, $Co_5(OH)_6(SeO_4)_2$, and sometimes other related impurities such as the natrochalcite $NaCo_2(H_3O_2)(SeO_4)_2$.[14] To obtain **1H** or **1D** as the major phase requires the following experimental optimized conditions: (a) limit the reaction temperature to 150 °C, (b) reaction time should be set to 48 h, (c) use boiled deoxygenated distilled water to avoid the oxidation of Co(II), and (d) most importantly, use a NaOH/Co ratio less than 0.6 instead of the stoichiometric 1.2 according to the chemical formula. These conditions were less severe than those found suitable in the case of the corresponding sulfate, where the NaOH/Co was limited to 0.17 and the reaction time to 24 h.[9] Experiments in D_2O under the optimized conditions for the H_2O salt clearly promote the formation of an increased amount of secondary phases. Some phases crystallize as dark red colored microcrystals. For measurements that need only a few milligrams such as for magnetization using a SQUID, it was possible to eliminate part of these secondary phases under a microscope. On the other hand, neutron diffraction requires a few grams,

(8) Kurmoo, M. *Metal−Organic and Organic Molecular Magnets*; Day, P., Underhill, A. E., Eds.; Special Publication, Royal Society of Chemistry: Cambridge, U. K., 2000; vol. *252*, p 185.

(9) (a) Ben Salah, M.; Vilminot, S.; André, G.; Richard-Plouet, M.; Bourée-Vigneron, F.; Mhiri, T.; Takagi, S; Kurmoo, M. *J. Am. Chem. Soc*. **2006**, *128*, 7972. (b) Ben Salah, M.; Vilminot, S.; Richard-Plouet, M.; André, G.; Mhiri, T.; Kurmoo, M. *Chem. Comm*. **2004**, 2548.

(10) (a) Vilminot, S.; André, G.; Richard-Plouet, M.; Bourée-Vigneron, F.; Kurmoo, M. *Inorg. Chem*. **2006**, *45*, 10938–10946. (b) Vilminot, S.; André, G.; Bourée-Vigneron, F.; Richard-Plouet, M.; Kurmoo, M. *Inorg. Chem*. **2007**, *46*, 10079.

(11) (a) Vilminot, S.; André, G.; Bourée-Vigneron, F.; Richard-Plouet, M.; Kurmoo, M. *Inorg. Chem*. **2007**, *46*, 10079. (b) Vilminot, S.; Richard-Plouet, M.; André, G.; Swierczynski, D.; Bourée-Vigneron, F.; Marino, E.; Guillot, M. *Cryst. Eng*. **2002**, *5*, 177. (c) Ben Salah, M.; Vilminot, S.; Mhiri, T.; Kurmoo, M. *Eur. J. Inorg. Chem*. **2004**, 2272. (d) Vilminot, S.; Richard-Plouet, M.; André, G.; Swierczynski, D.; Bourée-Vigneron, F.; Kurmoo, M. *Dalton Trans*. **2006**, 1455.

(12) Vilminot, S.; Richard-Plouet, M.; André, G.; Swierczynski, D.; Bourée-Vigneron, F.; Kurmoo, M. *Inorg. Chem*. **2003**, *42*, 6859.

(13) Rodriguez-Carvajal, J. *FULLPROF: Rietveld, Profile Matching and Integrated Intensity Refinement of X-Ray and/or Neutron Data*, 3.5d Version; Léon-Brillouin Laboratory/CEA Saclay: France, 2005.

(14) Vilminot, S.; André, G.; Bourée-Vigneron, F; Baker, P. J.; Blundell, S. J.; Kurmoo, M. *J. Am. Chem. Soc*. **2008**, *130*, 13490–13499.

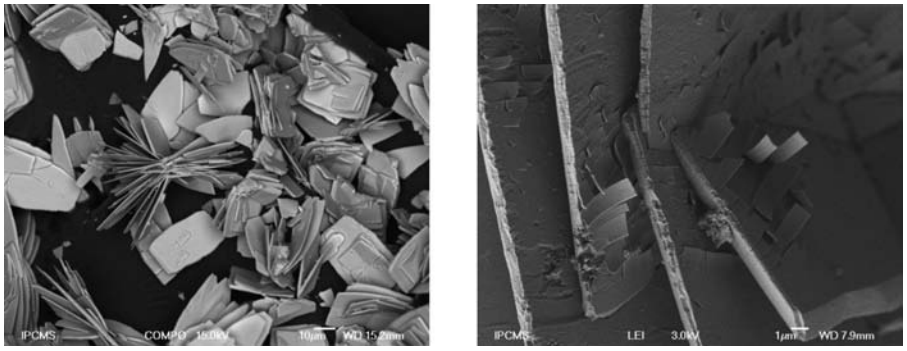

Figure 1. Electron micrographs of crystals of $Co_5(OH)_6(SeO_4)_2(H_2O)_4$: crystals under short unfocused (left) and long focused (right) periods of irradiation.

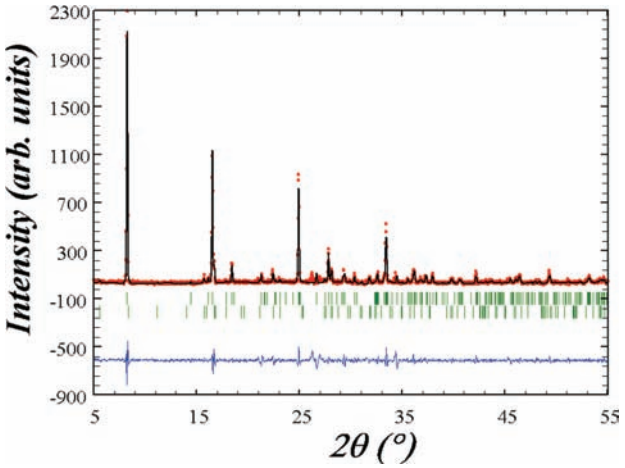

Figure 2. Pattern matching of the X-ray powder diffraction at 300 K of **1H**. The two sets of ticks correspond to those of **1H** (upper) and to the anhydrous salt (lower).

and therefore this large-scale purification was not possible. In order to try identifying the possible phases, SEM observations and EDX analyses have been performed on samples from few batches.

SEM Observations and EDX Analyses. Figure 1 shows a view at low magnification of a sample that appears homogeneous in color and crystal habit and with the X-ray diffraction pattern exhibiting primarily the Bragg reflections of **1H**. The crystals appear as platelets that can reach a few tens of micrometers. EDX analyses on different crystals give results in agreement with the **1H** formula: observed (calculated, atom%) Se, 9.4 (8); Co, 19.8 (20); O, 70.8 (72). Moreover, when the electron beam is focused on the crystals for a long period, they are damaged at the surface. The curving and flaking of the plates may be due to local heating resulting in the loss of water.

EDX analyses on a few crystals having a different habit led us to conclude a possible $NaCo_2(H_3O_2)(SeO_4)_2$ formulation. For the samples prepared with D_2O, SEM observations reveal the presence of other types of crystals.

X-Ray Powder Diffraction. The XRD patterns of **1H** and **1D** appear similar to the ones for the corresponding sulfate analogues. They are dominated by a progression of strong Bragg reflections based on 00*l* due to preferential orientations of the plate crystals in the Bragg−Brentano geometry used to record the data (Figure 2). Using the unit cell parameters for the sulfate, monoclinic system $P2_1/c$, their cell parameters have been refined by Le Bail pattern matching of the X-ray powder diffraction data with consideration of a contribution from the anhydrous salt. Therefore, **1H** and **1D** are assumed to be isostructural to their sulfate analogues. However, the full Rietveld refinements for the structures were hampered by the preferential orientation of the Bragg−Brentano geometry of the apparatus, though this is less of a problem for the neutron diffraction data (Table 1) where better averaging is possible. It is to be noted that the basic structural motif is correct as found by the Rietveld refinement of the neutron data at 12 K. As expected, the replacement of the sulfate ion (mean S−O = 1.48 Å) by the bigger selenate (mean Se−O = 1.65 Å) results in a shift of the 00*l* Bragg reflections toward lower 2θ values. While the *a* and *b* unit cell parameters remain constant on going from sulfate to selenate, the *c* axis increases by more than 4% from 20.547 to 21.436 Å.[9] The increase of the volume cell is therefore only due to the expansion along the *c* axis. This suggests that the layer is very rigid to whatever modifications are made in the gallery. The structure consists of edge-sharing octahedra within brucite layers having an anisotropic arrangement of chains of two (Co1 and Co2) of the three independent cobalt atoms along the *b* axis (Figure 3). The *ab* plane is the brucite layer that involves one oxygen atom of the SeO_4 in four hydroxides of $Co(OH)_2$. These layers are then bridged by the octahedra of the third cobalt atom (Co3) through the two-*trans* coordinated SeO_4, thus pillared by ...OXO_3−Co-$(H_2O)_4$−O_3XO... where X = S or Se. The increase of the *c* axis by about 0.22 Å per X−O bond is close to the expected 0.18 Å for replacing sulfate by selenate. The crystal system is not changed as a function of the temperature from 1.6 to 300 K, but there is a contraction of the lattice on cooling (V = 747 Å^3 at 300 K and 729 Å^3 at 1.6 K). While the *b* axis parameter is not altered on cooling, those of *a*, *c*, and

Table 1. Summary of the Rietveld Refinements at Different Temperatures for a Sample of **1D**

	XRD 300 K[a]	NPD 12 K[b]	NPD 1.6 K[b,c]
a (Å)	5.4958(14)	5.4473(12)	5.4226(13)
b (Å)	6.3447(11)	6.3428(9)	6.3475(10)
c (Å)	21.436(7)	21.248(4)	21.171(6)
β (deg)	92.06(3)	91.82(1)	90.78(2)
V (Å^3)	747.0(8)	733.8(5)	728.6(7)
R_p (%)	15.7	11.0	14.5
R_{wp} (%)	16.8	11.9	16.2
R_B (%)		4.01	6.01
R_F (%)		3.42	4.33

[a] Le Bail pattern matching. [b] Rietveld refinement. [c] R_{mag} = 8.58%.

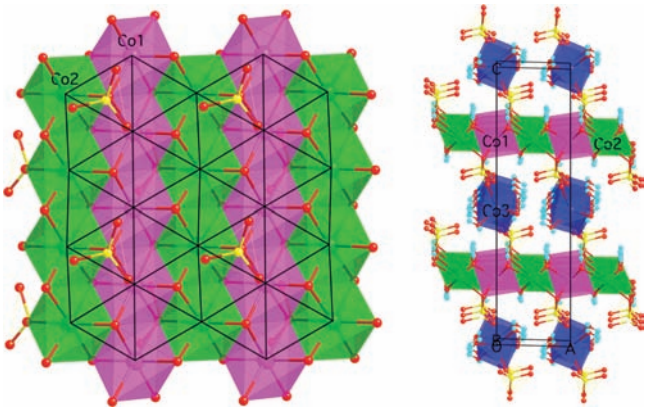

Figure 3. Views of the layered structure of $Co_5(OH)_6(SeO_4)_2(H_2O)_4$ showing the two different octahedral sites (left) within a layer and the way the layers are pillared by the $OSeO_3-Co(H_2O)_4-O_3SeO$ (right).

β are contracted by 1.3%. It is interesting to note that the magnetostriction is along the same contracted axes, while the b axis remains unaltered and is the easy axis of this ferromagnet (see below).

For most samples, extra Bragg reflections are present, and they are also made up of a progression of 00*l* Bragg lines characteristic of a layered structure (Figure 2). We believe they belong to an impurity phase consisting of the anhydrous form. These lines are related to those found for the equivalent anhydrous cobalt hydroxy-sulfate, for which the single crystal diffraction reveals a hexagonal system with unit cell parameters $a = 6.530(1)$ Å and $c = 32.05(3)$ Å.

Infrared Spectroscopy. The infrared spectra (Figure S1, Supporting Information) of **1H** and **1D** reveal the presence of two families of bands; one is related to O−H and H_2O vibrations that are shifted from **1H** to **1D** by a factor of around $(18/(17 \times 2))^{1/2}$, and the other is related to the SeO_4 tetrahedron vibrations that remain constant in position. In the 3600−3200 cm^{-1} (3000−2300 cm^{-1}) region, the five observed bands are attributed to OH(D) stretching vibrations. While the first three at 3602, 3557, and 3488 cm^{-1} (2690, 2629, and 2592 cm^{-1}) are sharp, the other two at 3333 and 3183 cm^{-1} (2469 and 2351 cm^{-1}) are broad. A similar result was evidenced in the case of the corresponding sulfate compounds, $Co_5(OH)_6(SO_4)_2(H_2O)_4$ and $Co_5(OD)_6(SO_4)_2(D_2O)_4$. According to the structural results that evidenced much shorter hydrogen bonds engaged by water molecules, the broad bands were attributed to $H(D)_2O$ stretching vibrations, whereas the sharp ones correspond to OH(D) vibrations.[15] It appears reasonable to draw the same conclusion concerning the selenate even if the structure determination is less precise. At 1615 cm^{-1} for **1H** (1192 cm^{-1} for **1D**), the band is related to the deformation of the water molecules. A broad band around 680 cm^{-1} in **1H** (498 cm^{-1} for **1D**) has been attributed to other OH modes. For the bands showing no deuteration effects, those at 889 and 865 cm^{-1} are attributed to the ν_3 of selenate, the presence of a doublet being in relation with the distorted local symmetry that also permits the ν_1 vibration to be IR active at 813 cm^{-1}.[15] The ν_4 mode is observed at 425 cm^{-1}. Very similar results were evidenced for the corresponding H and D sulfates.

(15) Nakamoto, K. *Infrared and Raman Spectra of Inorganic and Coordination Compounds*, 4th ed.; John Wiley & Sons: New York, 1986.

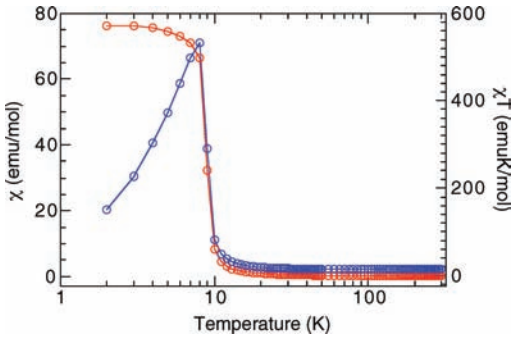

Figure 4. Temperature dependence of χ (red) and χT (blue) of $Co_5(OH)_6(SeO_4)_2(H_2O)_4$.

Thermal Properties. The TGA trace (Figure S2, Supporting Information) recorded under air reveals a four-step evolution of the sample weight. They correspond to water loss (170 to 260 °C $\Delta P/P = 7.5\%$, calc. = 9.5%), OH decomposition as H_2O (260 to 350 °C, $\Delta P/P = 8.9\%$, calc. = 7.2%), selenate ion decomposition as SeO_3 with concomitant oxidation of Co (350 to 730 °C, $\Delta P/P = 30.1\%$, calc. = 29.8%), and finally reduction of Co_3O_4 in CoO (910 to 925 °C, $\Delta P/P = 3.5\%$, calc. = 3.3%). Apparently the water loss and the OH decomposition are concomitant, since their sum (16.4%) is closer to the expected value (16.7%) than the individual values. The total weight loss, 48.9%, is close to the expected one, 50.5%, the difference being attributed to the impurities detected by powder X-ray diffraction and EDX analyses. The weight losses are accompanied by endothermal effects on the TDA trace at 222, 337, 474, and 920 °C.

Magnetic Properties. The temperature dependence of the magnetic susceptibility and its product with the temperature are shown in Figure 4. In the paramagnetic region, the susceptibility follows a Curie−Weiss law, $\chi = C/(T-\theta)$, with $C = 14.98(4)$ emu K/mol and $\theta = +3.2(5)$ K as deduced from a fit of $1/\chi$ versus the temperature data in the temperature region 150−300 K. The Curie constant translates to 2.996 emu K/mol of cobalt. From this value, we get an effective moment of 4.90 μ_B. This value is larger than expected assuming only the spin quantum numbers but is within the range observed for most Co(II) systems. For the corresponding sulfate, a value of 4.82 μ_B was observed. This enhancement is due to the presence of spin−orbit coupling. At low temperatures, the effective spin reduces to 1/2, and a virtual Weiss constant of −20 K has been proposed by Mabbs and Machin for noninteracting cobalt(II).[16] In our case, $\theta = +3.2(5)$ K characterizes ferromagnetic interactions between nearest Co neighbors due to the edge-sharing arrangement leading to Co−O−Co angles less than 98°, satisfying the Goodenough and Kanamori rule.[17,18]

At around 9 K, the susceptibility sharply increases, and it is accompanied by the presence of one peak for both the real and imaginary parts of the ac susceptibilities (Figure 5). According to the temperature of the maximum

(16) Mabbs, F. E.; Machin, D. J. *Magnetism and Transition Metal Complexes*; Chapman and Hall: London, 1973.

(17) Goodenough, J. B. *Magnetism and the Chemical Bond*; John Wiley and Sons: New York, 1963.

(18) (a) Kanamori, J. *J. Phys. Chem. Solids* **1959**, *10*, 87. (b) Kanamori, J. In *Magnetism*; Rado, G. T., Suhl, H., Eds.; Academic Press: New York, 1963; vol. *I*, ch. 4, p 127.

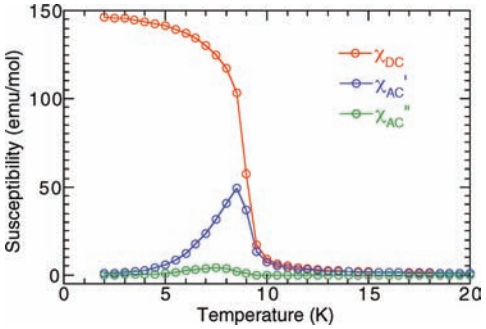

Figure 5. Temperature dependence of the ac (1 Oe, 17 Hz) and dc (FC, H = 1.6 Oe) susceptibilities of $Co_5(OH)_6(SeO_4)_2(H_2O)_4$ on cooling.

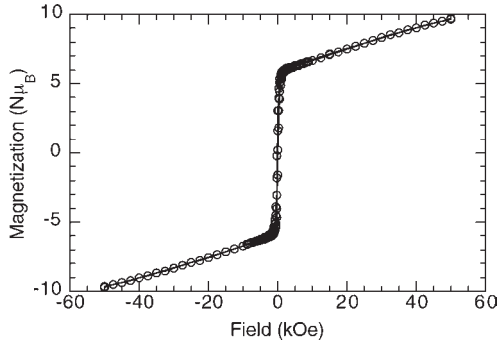

Figure 6. Isothermal magnetization of $Co_5(OH)_6(SeO_4)_2(H_2O)_4$ at 2 K.

of the peak of the real part and the nonzero imaginary component, the Curie temperature of the ferromagnet can be deduced as $T_C = 9$ K.

The isothermal magnetization at 2 K reveals a hysteresis loop with a remnant magnetization around 4 μ_B and a coercive field of 100 Oe (Figure 6). The magnetization at 50 kOe has a value of 9.65 μ_B, which indicates that all the moments are almost aligned with the field. This value is very close to the value for the corresponding sulfate, 9.67 μ_B.[9] The presence of very small crystals did not allow measurements on aligned samples as was possible for the sulfate compound.

Magnetic Structure Determination. A comparison of the neutron powder patterns recorded at 1.6 and 12 K (Figure 7), i.e., below and above T_C reveals a strong increase of the Bragg reflection at 13.10° indexed as (002). On the difference pattern, three other contributions clearly appear at 22.09°, 26.38°, and 39.98°. The last two can be attributed to (004) and (006) planes of **1D**, while the first one is attributed to an impurity peak (Figures S3 and S4, Supporting Information). The fact that no new lines appear compared to the pattern taken above the magnetic ordering temperature and that only an increase in intensity of some nuclear lines is observed is characteristic of a ferromagnetic structure.

The associated magnetic structure (Figure 8) has been determined employing Bertaut's representation analysis

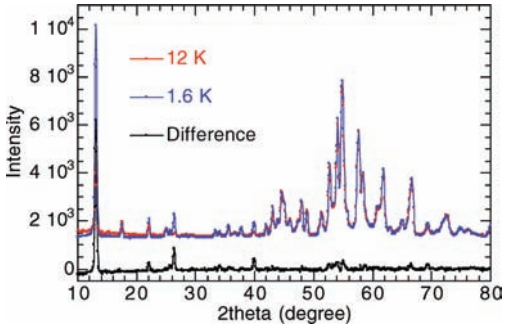

Figure 7. Observed neutron diffraction patterns of $Co_5(OD)_6(SeO_4)_2(D_2O)_4$ above (12 K, red) and below (1.5 K, blue) the magnetic ordering temperature (9 K) and the difference (black).

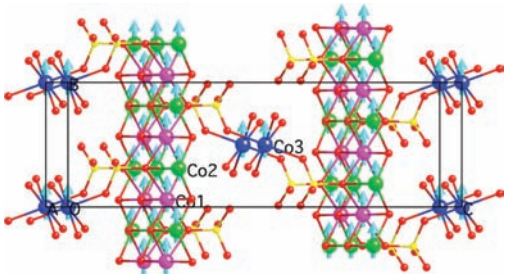

Figure 8. Magnetic structure of $Co_5(OD)_6(SeO_4)_2(D_2O)_4$.

method applied to the $P2_1/c$ space group with propagation vector $\mathbf{k} = (0, 0, 0)$ and Wyckoff positions (4e) for Co1 and Co2 and (2a) for Co3.[19−21] Four one-dimensional irreductible representations, Γ_1 to Γ_4, are evidenced for the (4e) position and only two Γ_1 and Γ_3 for (2a). Only Γ_1 and Γ_3 can describe a ferromagnetic structure, with the moments oriented along *b* and *a*, respectively. For Γ_3, a possible component of the moment along the *c* axis is theoretically possible, but refinement with the moment lying in the *ac* plane results in a value of zero for M_z. Consideration of the nuclear structure reveals that Co1 and Co2 belong to different chains running along the *b* axis within the brucite layers. The octahedra around Co1 and Co2 share corners with each other, and therefore it can be assumed that the pathways between Co1−Co1, Co2−Co2, and Co1−Co2 operate with exchange interactions of similar values. Furthermore, we can also assume that the magnetic moments are equal for Co1 and Co2. Interestingly, refinements with independent values for Co1 and Co2 severely diverge. Concerning the moment of Co3, three possibilities exist: (a) M(Co3) is equal to M(Co1) and M(Co2), (b) M(Co3) is independent of M(Co1) and M(Co2), and (c) M(Co3) = 0. The last model was adopted for the corresponding sulfate.[9] Table 2 summarizes the results.

From Table 2, it appears that, for the same model, alignment of the magnetic moment along the *b* axis gives a slightly better result than that along the *a* axis. Similar results are obtained with a nonzero value for M_y(Co3) either equal to M_y(Co1) = M_y(Co2) or independent from M_y(Co1) = M_y(Co2), with nearly the same $R_{magnetic}$ factors. However, refinements for data recorded at higher temperatures are all significantly worse for independent M_y(Co3). Therefore, the model with the same moment for the Co atoms has been selected. The last model with

(19) Bertaut, E. F. *Acta Crystallogr., Sect. A* **1968**, *24*, 217.
(20) KAREP−A Program for Calculating Irreductible Space Group Representations: Hovestreydt, E.; Aroyo, I.; Sattler, S.; Wondratschek, H. *J. Appl. Crystallogr.*, **1992**, *25*, 544.
(21) *BASIREPS−A Program for Calculating Non-Normalized Basis Functions of the Irreductible Representations of the Little Group Gk for Atom Properties in a Crystal*; Rodriguez-Carvajal, J., Ed.; Laboratoire Léon Brillouin (CEA(CNRS), CEA Saclay: Gif sur Yvette, France, 2004.

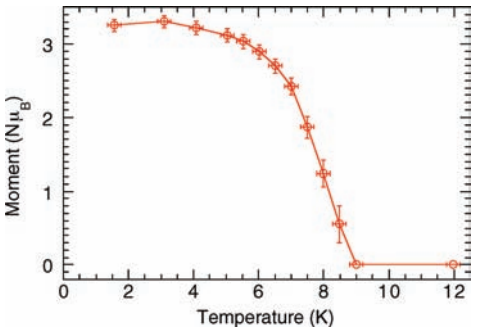

Figure 9. Temperature dependence of the moment per cobalt ion for $Co_5(OD)_6(SeO_4)_2(D_2O)_4$ derived from the neutron diffraction data.

Table 2. Results from the Rietveld Refinements of the Magnetic Structures of **1D**

M_x(Co1, Co2, Co3) (μ_B)	M_y(Co1 and Co2) (μ_B)	M_y(Co3) (μ_B)	$R_{magnetic}$ (%)
3.21(9)			10.29
	3.25(8)	3.25(8)	8.59
	3.23(9)	2.8(7)	8.62
	3.00(8)	0	9.69

M_y(Co3) = 0 has a slightly higher $R_{magnetic}$ value. In the case of the sulfate, the same model with M_y(Co3) being independent from M_y(Co1) = M_y(Co2) yielded M_y = 0.184(368) μ_B for Co3, and therefore it was considered that the moment of Co3 was random.[9] It is interesting to note that the moments are aligned along the *b* axis in both compounds, which corresponds to the chain direction of the anisotropic layer (Figure 8). The moment for the three Co atoms, 3.25(8) μ_B (3.33(3) μ_B for the sulfate), is slightly higher than the 3 μ_B expected for Co(II), and it is explained by a contribution of orbital moments. Refinement of the data collected between 3 and 8.5 K shows that the same magnetic structure is observed for all temperatures below T_C. The corresponding temperature dependence of the M_y component of Co1 = Co2 = Co3 is reported in Figure 9. The moment gradually decreases from 1.6 K down to 9 K where it becomes zero.

A further observation in the neutron diffraction experiments is the occurrence of an increased background at low angles that may be associated with short-range magnetic ordering. The background is almost constant and weak between 1.6 and 7 K. It increases to a maximum at the Curie temperature (Figure S5, Supporting Information). The intensity above the Curie temperature suggests that there is already short-range order of a reasonable length, while the decrease at low temperatures may be interpreted as an increase of the diffraction volume of the long-range order at the expense of that of the short-range ordering. Further work will be needed to fully characterize this effect. However, the short-range ordering appears to be antiferromagnetic and does not adopt the same crystal system as found in the case of $M_3(OH)_2(SO_4)_2(H_2O)_4$, M = Co and Mn.[22,23]

Conclusion

The reaction conditions for the formation of pure $Co_5(OH)_6(SeO_4)_2(H_2O)_4$ appear to be slightly different from those of $Co_5(OD)_6(SeO_4)_2(D_2O)_4$ and even more different from those of the sulfate analogues. All of these compounds are stable and isostructural for all temperatures between 2 and 300 K. Their magnetic properties are those of ferromagnets with Curie temperatures of 9 K (selenate, d_{00l} = 10.72 Å) and 14 K (sulfate, d_{00l} = 10.27 Å). The Curie temperature correlates well with the established linear relation with the content (number of tetrahedral to octahedral sites) within each layer in the case of X-ray determined structures.[5] The moments lie along the *b* axis, that is, one of the anisotropic axes of the layer or along the chains of Co1 and Co2, in both cases.

Acknowledgment. This work was funded by the CNRS (France) and the CEA (France).

Supporting Information Available: Infrared spectra, TG-DTA, and neutron diffraction at different temperatures. This material is available free of charge via the Internet at http://pubs.acs.org.

(22) Ben Salah, M.; Vilminot, S.; André, G.; Richard-Plouet, M.; Mhiri, T.; Kurmoo, M. *Chem. Mater.* **2005**, *17*, 2612.
(23) Ben Salah, M.; Vilminot, S.; André, G.; Richard-Plouet, M.; Bourée-Vigneron, F.; Mhiri, T.; Kurmoo, M. *Chem. Eur. J.* **2004**, *10*, 2048.